

Photochemistry of High-Spin Iron(III) Complexes of the Macrocyclic Ligands [15]pydieneN₅ and [15]pyaneN₅. An Investigation of the Charge-Transfer Processes

G. FERRAUDI

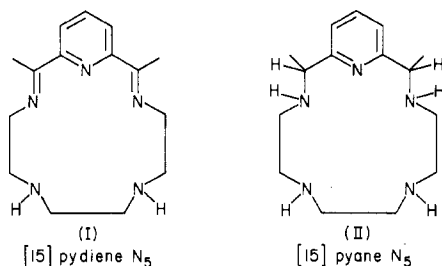
Received March 9, 1979

The charge-transfer photochemistries of iron(III) complexes of the [15]pydieneN₅ and [15]pyaneN₅ ligands were investigated in nonaqueous media. The photochemical reactivity, exhibited by these compounds, can be described as a reduction of the metal center with a concurrent oxidation of axially coordinated ligands—Cl⁻, Br⁻, N₃⁻, NCS⁻, I⁻. Intermediates, produced in these reactions, were investigated by flash photolysis and intercepted with appropriate scavengers. Threshold energies for photochemical reactivity obtained for Fe([15]pydieneN₅)(X)₂⁺ (X: Cl⁻, Br⁻, N₃⁻, NCS⁻) and Fe([15]pyaneN₅)(X)₂⁺ (X: Cl⁻, Br⁻, N₃⁻) exhibited a large dependence on both the macrocyclic and the axially coordinated ligands.

Introduction

Although the photochemistry of iron(III) species has been largely investigated,¹⁻¹² studies with complexes of macrocyclic ligands have not been initiated until recently.^{6,9} Results available up to this work suggest that the photooxidation of the ligands coordinated in axial positions can be one of the most significant reaction modes.⁹ In addition, a different photochemical reactivity—photooxidation of the solvent—has been claimed for photolyses of Fe(phen)₃³⁺.⁵ However, more recent evidence shows that the photooxidation of the 1,10-phenanthroline ligand with a concurrent reduction of the metal center can be a better description of the primary process.⁴

The photochemical properties of iron(III) complexes have been attributed to the population of ligand to metal charge-transfer states.¹ However, parallel trends in photochemical and spectroscopic properties have not been fully established. Closely related iron(III) compounds of the macrocycles [15]pydieneN₅ (I) and [15]pyaneN₅ (II) have been used



throughout this work.¹³ Several factors that may have influence upon the photochemistry of iron(III) species, namely, the electroaffinity of the radical formed in the oxidation of the axial ligand and structural features of the macrocycles, have been investigated here.

Experimental Section

Photochemical Procedures. A description of the flash-photolysis apparatus was given elsewhere.¹⁴ Although most of the experimental setup used for flash irradiations was not modified, several features were added in order to improve its resolution in kinetic and spectrometric measurements. The phototube output was filtered through RC filters with time constants appropriate to the experiment. The filtered signals formed the vertical inputs of a storage 507 Tektronix scope and a Biomation 805 waveform recorder. Finally, the digitized output of the waveform recorder was fed either into a logarithmic amplifier-strip chart recorder or directly into the strip chart recorder. The branch of the logarithmic amplifier gave a record of the function $\Delta A = \log V_t - \log V_0$, where V_0 and V_t are the phototube outputs before and at a time t after the flash irradiation.

A 300-W UV Eimac xenon lamp, combined with condensing lenses and a high-intensity Bausch and Lomb monochromator, was used for continuous-wave irradiations. The quasi-monochromatic light exhibited a Gaussian distribution of the intensity with 10-nm half-bandwidth. In addition, some 254-nm irradiations were carried out with a G 4T4-1 GE low-pressure mercury lamp. The light intensities were measured with tris(oxalato)ferrate(III) and Reinecke salt.^{15,16}

Solutions of the complexes were irradiated in cells with a slab geometry and 1-cm optical path. Additional features were introduced in these cells for both electrochemical and optical investigations of the photochemical processes (see Figure 1).

Oxygen was removed from the photolyte solutions with streams of solvent-saturated argon. The deaerated liquids were handled in a gastight apparatus.

Electrochemical Procedures. Cyclic voltammetry was performed with an instrumental setup built in this laboratory. A triangular-wave generator was used with an adder; voltage and current followers and a lock-in amplifier were used for phase-sensitive detection as described elsewhere.¹⁷ A platinum wire and a platinum gauze were respectively used as auxiliary and working electrodes for the cell. A chloride-coated silver wire immersed in AgCl-saturated acetonitrile or a silver wire in contact with 0.1 M AgNO₃ in acetonitrile was used as a reference electrode, third electrode, for different experiments.¹⁸ The reference electrode was separated from the solutions by a salt bridge which contained either 0.1 M Et₄NBr or 0.1 M Et₄Cl in acetonitrile.¹⁹ Compartments of the cell were isolated from each other by means of medium glass frits.

Values of $E_{1/2}$ were obtained from cyclic voltammograms by means of the relationship $1/2(E_p + E_{p/2}) = E_{1/2}$, between the potential for a maximum diffusion current, E_p , and the potential for a half of the

- (1) Balzani, V.; Carassiti, V. "Photochemistry of Coordination Compounds"; Academic Press: New York, 1970.
- (2) David, P. G.; Wehry, E. L. *Mol. Photochem.* **1973**, *5*, 21.
- (3) Chen, C. N.; Lichtin, N.; Stein, G. *Science* **1975**, *190*, 879.
- (4) Malik, G. M.; Laurence, G. S. *Inorg. Chim. Acta* **1978**, *28*, L149.
- (5) Wehry, E. L.; Ward, R. A. *Inorg. Chem.* **1971**, *10*, 2660.
- (6) Yu, C.; Chiang, T. L.; Yu, L.; King, E. T. *J. Biol. Chem.* **1975**, *250*, 618.
- (7) Miessler, G. L.; Stuk, G.; Smith, T. P.; Given, K. W.; Palazzotto, M. C.; Pignolet, L. H. *Inorg. Chem.* **1976**, *15*, 1982.
- (8) Cooper, G. D.; DeGraff, B. A. *J. Phys. Chem.* **1971**, *75*, 2918; **1972**, *76*, 2818.
- (9) Reichgott, D. W.; Rose, N. J. *J. Am. Chem. Soc.* **1977**, *99*, 1813.
- (10) Incorvia, M. J.; Zink, J. I. *Inorg. Chem.* **1978**, *17*, 2250.
- (11) Liu, P. H.; Zink, J. I. *J. Am. Chem. Soc.* **1977**, *99*, 2155.
- (12) Schwendiman, D. P.; Zink, J. I. *J. Am. Chem. Soc.* **1976**, *98*, 4439.
- (13) Abbreviations: [15]pydieneN₅, 2,13-dimethyl-3,6,9,12,18-pentaazabicyclo[12.3.1]octadeca-1(18),2,12,14,16-pentaene; [15]pyaneN₅, 2,13-dimethyl-3,6,9,12,18-pentaazabicyclo[12.3.1]octadeca-1(18),14,16-triene.

(14) Ferraudi, G. *Inorg. Chem.* **1978**, *17*, 1741.(15) Hatchard, C. G.; Parker, C. A. *Proc. R. Soc. London, Ser. A* **1956**, *235*, 518.(16) Wegner, E. E.; Adamson, A. J. *Am. Chem. Soc.* **1966**, *88*, 394.

(17) Diefenderfer, A. J. "Principles of Electronic Instrumentation"; W. B. Saunders: Philadelphia, 1972; pp 550-8.

(18) The potential of the silver chloride electrode was -0.17 V vs. 0.1 M AgNO₃ in acetonitrile. Moreover, a reduction potential of $E^\circ \approx +0.92$ V vs. the standard hydrogen electrode was determined for 0.1 M AgNO₃ in acetonitrile.(19) Potentials, determined in solutions with either Li⁺ or Et₄N⁺ as cations of the support electrolyte, exhibited no differences beyond the experimental error (± 20 mV).

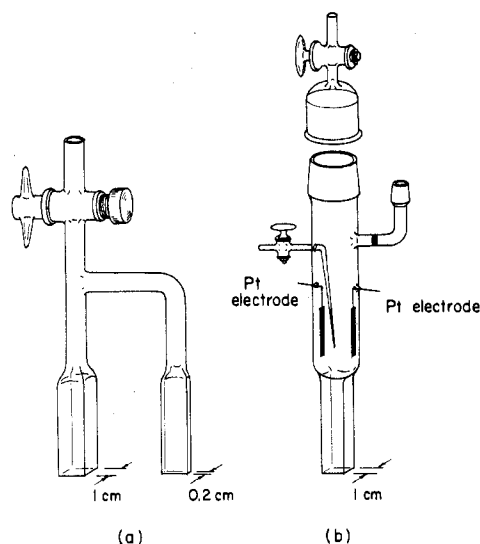


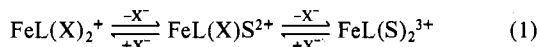
Figure 1. Cells used for spectroscopic (a) and electrochemical (b) investigation of the products produced in continuous-wave photolyses.

maximum diffusion current, $E_{p/2}$.

The electromotive force of the cells was measured either by potentiometry or with a high-impedance Chemitrex pH meter. The same methods were used for photogalvanic experiments, where a silver chloride electrode (see above) was used as a reference electrode.

Constant-potential electrolyses were carried out with an experimental setup that was described elsewhere.¹² Coulometric n values were determined from integration of the current-time curves obtained in controlled-potential electrolyses.

Analytical Procedures. Concentrations of the iron(III) complexes were determined for various periods of the irradiation by means of the near-ultraviolet absorbances. Changes in the spectra of the solutions were produced by a displacement of the anation equilibria, eq 1, when photochemically generated halide or pseudohalide radicals were trapped by appropriate vinyl or polyene monomers.^{1,20,21}



Several vinyl monomers, 2,5-dimethyl-1,5-hexadiene, *trans*-1,2-dimethyl-1,4-pentadiene, ethylene, and acrylonitrile, were used as scavengers throughout this work in order to confirm that the photochemical properties, measured for each complex, were independent of the scavenger(s).²¹ In this regard, energy thresholds for photochemical reactivity were calculated as an average of the values obtained with various scavengers.

The formation of iron(II) complexes was followed by potentiometry and by means of the absorption spectrum in experiments where 2-propanol was used as a radical scavenger. Also, the concentration of the reduced complex was determined by internal electrolysis. The compartment with the reduced complex was coupled by means of a salt bridge (see above) to the cathode. Either a silver chloride electrode (see above) or a platinum wire immersed in an aqueous solution of ferric ions (0.02 M $\text{Fe}(\text{ClO}_4)_3 \cdot 7\text{H}_2\text{O}$ in 0.1 M HClO_4) was used as a cathodic half-cell for these experiments. Concentrations of iron(II) were determined with 1,10-phenanthroline.

Materials. $[\text{Fe}_2([\text{15}]\text{pydieneN}_5)_2\text{O}](\text{ClO}_4)_4$, $[\text{Fe}([\text{15}]\text{pydieneN}_5)(\text{X}_2)]\text{ClO}_4$ (X: Cl^- , Br^- , I^- , NCS^-), and $[\text{Fe}([\text{15}]\text{pydieneN}_5)(\text{X})_2]\text{ClO}_4$ (X: Cl^- , Br^- , N_3^-) were synthesized by procedures reported in the literature.²²⁻²⁴ Two or three recrystallizations of the heptacoordinated diacido compounds were carried out from solutions

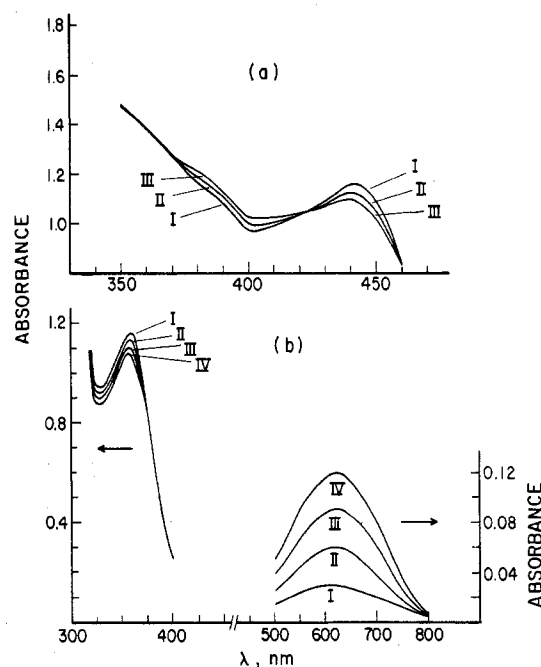


Figure 2. Spectral changes observed in continuous-wave photolyses. (a) $\text{Fe}([\text{15}]\text{pydienN}_5)\text{Br}_2^+$ photolyses in presence of 2.0 M 2,5-dimethyl-1,5-hexadiene, with excitations at 300 nm ($I_0 = 1.6 \times 10^{-4}$ einstein/(L·min)): (I) 0 s; (II) 560 s; (III) 1120 s. (b) $\text{Fe}([\text{15}]\text{pydieneN}_5)\text{Cl}_2^+$ photolyses in presence of 3.0 M 2-propanol, with excitations at 254 nm ($I_0 = 1.8 \times 10^{-4}$ einstein/(L·min)): (I) 0 min; (II) 5 min; (III) 10 min; (IV) 15 min. Absorbances determined with 2-mm optical path in (a) and left curve in (b).

of the corresponding lithium halides (0.1–0.01 M) in acetonitrile by the addition of sodium perchlorate.²⁴ The absorption spectra of these complexes agreed with previous reports.

$[\text{Fe}([\text{15}]\text{pydieneN}_5)(\text{N}_3)_2]\text{ClO}_4$ was synthesized by reacting $[\text{Fe}([\text{15}]\text{pydieneN}_5)_2(\text{ClO}_4)_2\text{O}](\text{ClO}_4)_2$ with sodium azide. **Caution!** Perchlorates and azides in contact with organic substances are potential explosives and must be handled with appropriate precautions. The dimeric iron(III) complex (2 g) and sodium azide (2 g) were dissolved in warm acetonitrile. The precipitation was induced by adding solid NaClO_4 in small fractions. The complex was recrystallized from 0.01 M LiN_3 in acetonitrile. Anal. Calcd: Fe, 15.92; N, 37.62. Found: Fe, 15.95; N, 37.30.

Acetonitrile and 2-propanol were of spectroquality grade and were used without further purification. Other chemicals, used throughout this work, were AR reagent grade.

Results

A. General Photochemical Features. Continuous-wave irradiations of iron(III) macrocyclic complexes ($\text{Fe}([\text{15}]\text{pydieneN}_5)(\text{X})_2^+$ (X: Cl^- , Br^- , N_3^- , NCS^-) in the absence of appropriate scavengers failed to produce permanent spectral changes. However, irradiations of the complexes in the presence of vinyl monomers produce a decrease of the absorbances in the region of the charge-transfer bands ($\text{X}^- \rightarrow \text{Fe}(\text{III})$; see below) and some increase at wavelengths shorter than or equal to 400 nm (see for example Figure 2a) for the bromide complex. The same differences were detected between the spectra of $\text{Fe}([\text{15}]\text{pydieneN}_5)(\text{X})_2^+ - \text{Fe}([\text{15}]\text{pydieneN}_5)_2\text{O}^{2+}$ mixtures and the spectrum of $\text{Fe}([\text{15}]\text{pydieneN}_5)(\text{X})^{2+}$. Moreover, the changes of the absorption spectra induced by irradiation disappear when halides (X: Cl^- , Br^-) or pseudohalides (X: N_3^- , NCS^-) were added in small amounts to the irradiated solutions. This behavior demonstrates that eq 1 is shifted as a consequence of the overall photoreaction.²⁰

Complexes of the [15]pyaneN₅ ligand, $\text{Fe}([\text{15}]\text{pyaneN}_5)(\text{X})_2^+$ (X: Cl^- , Br^- , N_3^-), exhibited the same qualitative behavior of the homologous [15]pydieneN₅ species for ultraviolet and visible irradiations.

(20) The irreversible addition of the radicals to the scavenger(s) double bond(s),^{1,21} followed by oxidation of the iron(II) species, displaces the position of the equilibria (eq 1).

(21) Henkins, A. D. In "Advances in Free Radical Chemistry"; Williams, G. H., Ed.; Academic Press: New York, 1965.

(22) Nelson, S. M.; Busch, D. H. *Inorg. Chem.* **1969**, *8*, 1859.

(23) Rakowski, M. C.; Rychek, M.; Busch, D. H. *Inorg. Chem.* **1975**, *14*, 1194.

(24) Configurations of a pentagonal bipyramid were found in complexes of the [15]pydieneN₅ ligand: Fleischner, E.; Hawkinson, S. *J. Am. Chem. Soc.* **1967**, *89*, 720. Similar configurations were assigned to complexes of [15]pyaneN₅.²³

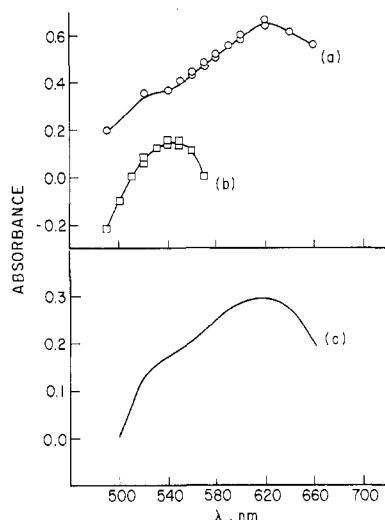


Figure 3. Transient spectra obtained in flash irradiations of $\text{Fe}([\text{15}]\text{pydieneN}_5)\text{Br}_2^+$ in deaerated CH_3CN : spectra determined at zero reaction time (a) in presence of 10^{-2} M allyl alcohol and (b) in 4×10^{-3} M HBr; spectrum of the reduction product (c) obtained for electrolyses of $\text{Fe}([\text{15}]\text{pydieneN}_5)\text{Br}_2^+$ in deaerated acetonitrile.

Irradiations of $\text{Fe}([\text{15}]\text{pydieneN}_5)(\text{X})_2^+$ ($\text{X}: \text{Cl}^-, \text{Br}^-$) were also carried out in deaerated solutions which contain 2-propanol (1.0–6.0 M) as a radical scavenger.²⁵ New absorbances between 600 and 800 nm (Figure 2b) were developed upon irradiation at wavelengths of the charge-transfer bands (see below). The broad absorption maximum is placed at 650–670 nm, and it has the extinction ϵ (1.0 ± 0.2) $\times 10^3 \text{ M}^{-1} \text{ cm}^{-1}$ for the irradiation product of $\text{Fe}([\text{15}]\text{pydieneN}_5)\text{Cl}_2^+$ (see Figure 2). Extinctions with the same order of magnitude, $\epsilon \sim 10^3 \text{ M}^{-1} \text{ cm}^{-1}$, were also measured for photolyses of the $\text{Fe}([\text{15}]\text{pydieneN}_5)\text{Br}_2^+$ (see Figure 3). Moreover, these reaction products exhibited a large reactivity toward oxygen. The spectra of the irradiated solutions were, after oxidation with oxygen, the same as those of the nonirradiated blanks.²⁶ In this regard the reaction products were assigned as iron(II) complexes of the macrocyclic ligand [15]pydieneN₅ (see below).

B. Flash Photolysis. Solutions of $\text{Fe}([\text{15}]\text{pydieneN}_5)(\text{X})_2^+$ ($\text{X}: \text{Cl}^-, \text{Br}^-, \text{N}_3^-, \text{I}^-$) in deaerated acetonitrile were flash photolyzed at wavelengths of the charge-transfer bands. Each of these complexes exhibited distinctive photochemical properties which are reported below.

Flash irradiations of 10^{-4} M $\text{Fe}([\text{15}]\text{pydieneN}_5)\text{Cl}_2^+$ or 10^{-4} M $\text{Fe}([\text{15}]\text{pydieneN}_5)\text{Br}_2^+$ in acetonitrile did not generate new absorbances with a life longer than or equal to 30 μs .²⁷ However, products of the irradiations, with absorption at 480–700 nm, were detected in solutions, where 2-propanol or allyl alcohol was used as a scavenger of the primary generated radicals. The results obtained in flash irradiations of $\text{Fe}([\text{15}]\text{pydieneN}_5)\text{Br}_2^+$ are shown in Figure 3. The same absorption spectrum was obtained for the photolysis product and the product of the electrochemical reduction (see Figure 3a,c and section D).

Also, $\text{Fe}([\text{15}]\text{pydieneN}_5)\text{Br}_2^+$ was flash irradiated in deaerated solutions of HBr (or LiBr) in acetonitrile. Tran-

- (25) Some dissociation of the diacido complexes (eq 1) was observed in solutions with a high 2-propanol concentration. However, such a dissociation was repressed with small concentrations of the appropriate lithium halides (5×10^{-2} M).
- (26) Oxidation of the ligand by oxygen²³ was observed as a slow reaction at times longer than those required for the oxidation of iron(II) species.
- (27) The reoxidation of the iron(II) product was observed with $t_{1/2} \approx 50$ ns in laser flash photolyses of $\text{Fe}([\text{15}]\text{pydieneN}_5)\text{Br}_2^+$ in acetonitrile: Ferraudi, G., unpublished observations.

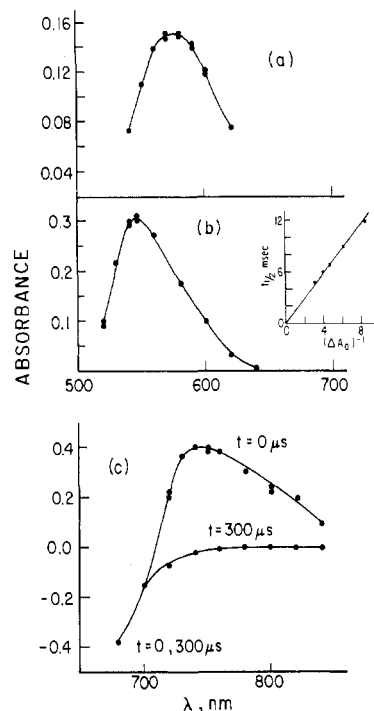


Figure 5. Spectra obtained for a zero reaction time in flash irradiations of $\text{Fe}([\text{15}]\text{pydieneN}_5)(\text{X})_2^+$ ($\text{X}: \text{N}_3^-$ (a), NCS^- (b), I^- (c)). Insert to (b) shows the dependence of the transient spectrum half-life on the reciprocal of the absorbance at zero reaction time, ΔA .

sients, generated for irradiations of 10^{-4} M $\text{Fe}([\text{15}]\text{pydieneN}_5)\text{Br}_2^+$ in 3.3×10^{-3} M HBr, did no longer present the maximum absorption at 620 nm (Figure 3b). Moreover, the formation ($t_{1/2} = (1.3 \pm 0.2) \times 10^{-3}$ s) and the decay ($t_{1/2} = (2.7 \pm 0.2) \times 10^{-1}$ s) of the transient absorbances were well separated in time. The dependence of these processes on Br^- concentration suggests that they are related to a relaxation of the anation equilibria, eq 1.

The amount of the photoreduced complex, produced in flash irradiations of $\text{Fe}([\text{15}]\text{pydieneN}_5)\text{Br}_2^+$, increased with scavenger concentrations (Figure 4a) and with the number of pulses (Figure 4b).²⁸ Although the absorbance had a linear dependence on the number of flashes (Figure 4b), deviations were observed when the concentration of iron(III) complex was depleted by excessive irradiations.

Flash photolyses of $\text{Fe}([\text{15}]\text{pydieneN}_5)(\text{N}_3)_2^+$ in deaerated acetonitrile produced an increase of the solution absorbances with a maximum at 580 nm (see Figure 5a). These absorbances, generated during the irradiation, exhibited a nonlinear dependence with the number of pulses (Figure 4c).²⁸ The product of this irradiation is stable in the absence of oxygen. However, oxidation with air, followed by addition of NaN_3 in small amounts, gave a solution with the same absorption spectrum of the nonirradiated blanks.

A transient spectrum with a maximum absorption at 550 nm was obtained for flash irradiations of 10^{-4} M $\text{Fe}([\text{15}]\text{pydieneN}_5)(\text{NCS})_2^+$ in deaerated acetonitrile (Figure 5b). The decay process, investigated at 580 nm by varying the flash output between 250 and 40 J/pulse, exhibited a good second-order dependence in transient concentration (see insert to Figure 5b). A rate constant to extinction coefficient ratio, $k/\epsilon = 1.4 \times 10^4 \text{ cm}^{-1} \text{ s}^{-1}$, was obtained from these measurements.

Solutions of $\text{Fe}([\text{15}]\text{pydieneN}_5)\text{I}_2^+$ were irradiated at wavelengths longer than 280 or 320 nm, where there was no

(28) Supplementary material.

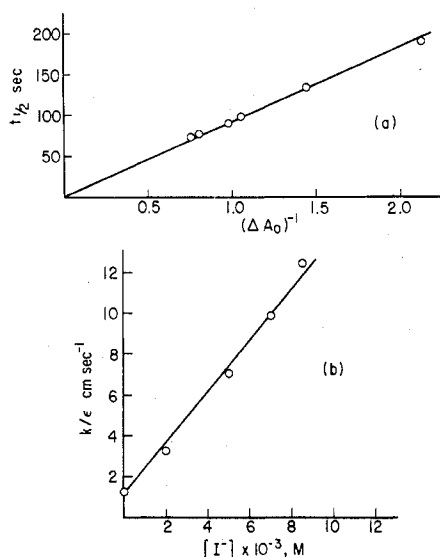


Figure 6. Second-order dependence of the half-life for transient absorbances generated in flash irradiations of $\text{Fe}([\text{15}]\text{pydieneN}_5)_2^+$ (a) (ΔA_0 = absorbance change determined at zero reaction time) and variation of the ratio of the second-order rate constant to the extinction coefficient, k/ϵ , with iodide concentration (b). Determinations for (a) and (b) were carried out at 760 nm.

significant absorption of light by the solvent (10^{-2} – 10^{-4} M NaI in acetonitrile). Although the absorptivities of the iron(III) complex were too large for wavelengths shorter than 650 nm, a transient spectrum, $\lambda_{\text{max}} \sim 740$ nm, was obtained for observations in the region of the 700–900 nm (Figure 5c). The initial spectrum decay was by a complex route which does not leave a permanent difference between the spectra of irradiated and blank solutions (see Figure 5c). An investigation of the reaction was carried out at 680 nm and 750 nm (Figure 6). The shortest lived decay of the absorbance at 750 nm (see Figure 5c) obeys a first-order rate law with a rate constant $k = 2.3 \times 10^4 \text{ s}^{-1}$. In addition, the amount ΔA_0 of the 680-nm absorbance, bleached during the life of the flash, presents the second-order dependence in flash energy, E , shown in eq 2 (see also Appendix I).

$$\Delta A_0 = [(9.0 \pm 0.2) \times 10^{-3}]E - [(1.4 \pm 0.3) \times 10^{-5}]E^2 \quad (2)$$

$40 < E < 250 \text{ J/flash}$

The recovery of the absorbance exhibited a second-order dependence on the amount of the absorbance bleached (Figure 6a). This second-order rate law is also obeyed in solutions, where iodide ions are present in various concentrations. However, the ratio of the rate constant to the extinction coefficient, k/ϵ , depends linearly on the iodide ion concentration (see Figure 6b and Appendix I).

The behavior of $\text{Fe}([\text{15}]\text{pyaneN}_5)(\text{X})_2^+$ (X: Cl^- , Br^- , N_3^-) in flash irradiations exhibited the same features already reported for the homologous $[\text{15}]\text{pydieneN}_5$ complexes.

C. Photovoltammetry and Photocoulometry. Solutions of $\text{Fe}([\text{15}]\text{pydieneN}_5)_2^+$ (2.0×10^{-4} M) in 2-propanol-acetonitrile solutions (0.2–0.8 M 2-propanol and 0.1 M LiCl) were irradiated for various periods at 254 nm ($I_0 = 1.8 \times 10^{-4}$ einstein/(L·min)). The photochemical reaction was followed by means of the redox potential of an electrochemical cell. The cell cathode was a silver chloride electrode, and the anode was a platinum wire immersed in irradiated solutions. The change of the redox potential, ΔV , exhibited a linear dependence on the logarithm of the irradiation time (Figure 7). This behavior can also be described by eq 3, where t is the irradiation period at 254 nm (see also Appendix II).

$$\Delta V = 0.180 - 0.058 \log t \quad (3)$$

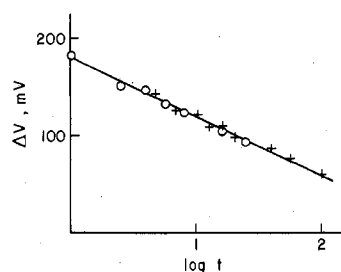


Figure 7. Variation of the electrochemical potential of the cell $\text{Fe}(\text{III})|\text{Fe}(\text{II})||\text{Ag}|\text{AgCl}$ with the logarithm of the irradiation time. The photochemical reaction of $\text{Fe}([\text{15}]\text{pydieneN}_5)_2^+$ was carried out by 254-nm irradiation of the complex in 1 M 2-propanol (see also Appendix II).

Table I. Electrochemical Data for Some Fe(III) Complexes of the $[\text{15}]\text{pydieneN}_5$ and $[\text{15}]\text{pyaneN}_5$ Ligands

| complex | $E_{1/2}, ^a \text{ V}$ | |
|---|-----------------------------|---------------------------|
| | $\text{Ag} \text{Ag}^+{}^b$ | $\text{Ag} \text{ClAg}^c$ |
| $\text{Fe}([\text{15}]\text{pyaneN}_5)_2^+$ | 0.60 ^d | 0.43 |
| $\text{Fe}([\text{15}]\text{pydieneN}_5)_2^+$ | 0.42 | 0.25 |
| $\text{Fe}([\text{15}]\text{pydieneN}_5)_2\text{Br}_2^+$ | 0.41 | 0.24 |
| $\text{Fe}([\text{15}]\text{pydieneN}_5)(\text{NCS})_2^+$ | 0.41 | 0.24 |

^a Half-wave potentials for reduction of iron(III) complexes in acetonitrile. Solutions of lithium halides (0.1 M LiCl, LiBr, or LiNCS in CH_3CN) were used for salt bridges and as supporting electrolytes. ^b Values obtained vs. a $\text{Ag}|0.1 \text{ M Ag}^+ (\text{CH}_3\text{CN})$ reference electrode. (See the Experimental Section.) ^c Values obtained vs. a $\text{Ag}|\text{ClAg} (\text{CH}_3\text{CN})$ reference electrode. (See the Experimental Section.) ^d A value $E_{1/2} = 0.56 \text{ V}$ was previously reported by Busch et al.²³

A redox potential, $V^\circ = 0.58 \text{ V}$, was estimated for the hemicell with irradiated solution (see Appendix II). Such a potential was found to be in good agreement with half-wave potentials for $\text{Fe}(\text{III})|\text{Fe}(\text{II})$ couples which were obtained throughout this work (see below) and reported in ref 23.

In addition, internal electrolyses were carried out with solutions of $\text{Fe}([\text{15}]\text{pydieneN}_5)_2^+$ which were irradiated for various periods at 254 nm (see below for other conditions). Ninety-eight percent of the reduced species, formed in these irradiations, was reoxidized. Integration of the current vs. time curves gave a total charge which is in good agreement with the amount of the photoreduced material; $9.65 \times 10^4 [\text{iron}(\text{II})]/(\text{charge}) = 0.97$.

D. Electrochemical Experiments. The cyclic voltammograms of $\text{Fe}([\text{15}]\text{pydieneN}_5)(\text{X})_2^+$ (X: Cl^- , Br^-) and $\text{Fe}([\text{15}]\text{pyaneN}_5)_2^+$ in acetonitrile indicate that $\text{Fe}(\text{III}) \rightarrow \text{Fe}(\text{II})$ reductions are reversible processes (Table I). In addition, differences equal to or smaller than 60 mV ($\Delta G < 1.5 \text{ kcal/mol}$) are observed between values of $E_{1/2}$ for complexes of the $[\text{15}]\text{pydieneN}_5$ and $[\text{15}]\text{pyaneN}_5$ ligands (Table I).

Controlled-potential electrolyses of $\text{Fe}([\text{15}]\text{pydieneN}_5)_2^+$ and $\text{Fe}([\text{15}]\text{pydieneN}_5)_2\text{Br}_2^+$ were carried out under various experimental conditions (0.1 M lithium halides in 0.1–2.0 M 2-propanol-acetonitrile mixtures). The absorption spectra of the electrolyzed solutions show new absorptions at 600–700 nm which are the same produced by continuous-wave photolyses (Figure 3). Oxidation of the solutions with air makes these new absorbances disappear. Moreover, integration of the current vs. time curves shows that this transformation is due to a one-electron reduction of the iron(III) complexes.

E. Quantum Yields. Irradiations of $\text{Fe}([\text{15}]\text{pydieneN}_5)_2^+$ were carried out in deaerated solutions, where 2-propanol (0.2–6.0 M 2-propanol in acetonitrile) was used as a radical scavenger. The yields for the photoreduction of this complex increased with 2-propanol concentration and did not show any dependence on the length of the irradiation for conversions smaller than 5% (see Table II).²⁸ Threshold energies for

Table III. Characteristic Energies^a for Charge-Transfer Absorptions and Charge-Transfer Photochemistries of Fe(III) Complexes with [15]pydieneN₅ and [15]pyaneN₅ Ligands

| X | f ^b | E _{abs} ^{max c} | E _{abs} ^{th d} | E _{phot} ^{th e} | E _{abs} ^{max} - E _{abs} th | E _{phot} th - E _{abs} th |
|---|----------------|-----------------------------------|----------------------------------|-----------------------------------|--|--|
| Fe([15]pydieneN ₅)(X) ₂ ⁺ | | | | | | |
| Cl ⁻ | 87 | 79.0 | 69.8 | 88.2 | 9.2 | 18.4 |
| Br ⁻ | 80 | 65.3 | 56.1 | 74.2 | 9.2 | 18.1 |
| N ₃ ⁻ | 69 | 58.5 | 49.3 | 66.0 | 9.2 | 16.7 |
| NCS | 49.9 | 58.4 | 49.3 | 54.0 | 9.1 | 4.7 |
| Fe([15]pyaneN ₅)(X) ₂ ⁺ | | | | | | |
| Cl ⁻ | 87 | f | >79.4 | >112 | | |
| Br ⁻ | 80 | 67.3 | 58.4 | 98.6 | 8.9 | 40.2 |
| N ₃ ⁻ | 40.9 | 60.6 | 52.0 | 87.0 | 8.6 | 35.0 |

^a Units are kcal/mol. ^b Electron affinity of the radical X[•]. Values obtained from: Page, F. M. *Adv. Chem. Ser.* **1962**, No. 36, 68; Blandamer, M. J.; Fox, M. J. *Chem. Rev.* **1970**, 70, 59; and references therein. ^c Energy for the maximum absorption in the first charge-transfer absorption band. ^d Threshold energy for charge-transfer absorption. Determined by extrapolation from the first charge-transfer absorption band. ^e Threshold energy for photoredox reactivity. ^f Not determined because of a large overlap with inner ligand transitions.

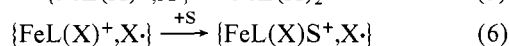
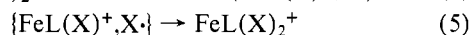
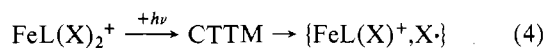
photochemical reduction were obtained from the dependence of the yields on photonic energy (Table III). Values for the thresholds, obtained in either 0.8 M 2-propanol ($E^{\text{th}} = 88.5$ kcal/mol) or 5.0 M 2-propanol ($E^{\text{th}} = 88.2$ kcal/mol), are in good agreement with each other.

Quantum yields for photochemical processes of Fe([15]pydieneN₅)(X)₂⁺ (X: Br⁻, N₃⁻, NCS⁻), determined by interception of the radicals with alkenes, present a marked dependence on the length of the irradiation.²⁹ The values, reported in Table II,²⁸ were evaluated from the slope of the concentration vs. time curves, extrapolated back to zero time. These yields increase with scavenger concentration as expected from flash-photolysis experiments (see Figure 4).²⁸ Threshold energies for photochemical reactivity (Table III) were obtained from the dependence of the yields on excitation energy for a given scavenger concentration (see Table II).²⁸

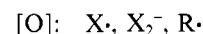
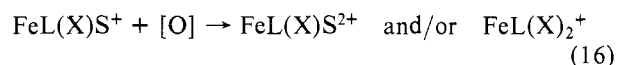
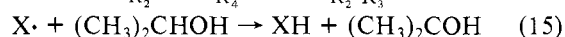
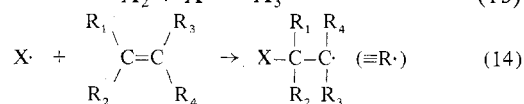
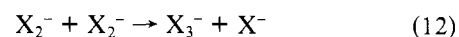
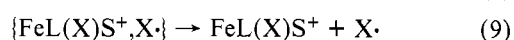
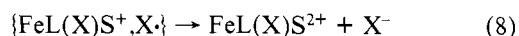
Quantum yields for Fe([15]pyaneN₅)(X)₂⁺ were obtained by using the same procedures used with the homologous [15]pydieneN₅ complexes (see above). The Fe([15]pyaneN₅)Cl₂⁺ complex has been found to be scarcely photoreactive for 254-nm irradiations (Table II).²⁸ Also, threshold energies for photoreduction of the [15]pyaneN₅ complexes were found to be larger than those of the corresponding [15]pydieneN₅ compounds (Table III).

Discussion

The photochemistries of Fe(III) complexes of the macrocyclic ligands (L) [15]pydieneN₅ and [15]pyaneN₅ can be described as an oxidation of the axially coordinated ligands and the reduction of the metal center. The observation of fast reactions between the products of the photoredox processes is in good agreement with reports on the reactivity of iron(II) complexes with radicals.¹ In this regard, the photochemical behavior of Fe([15]pydieneN₅)(X)₂⁺ (X: Cl⁻, Br⁻, N₃⁻, NCS⁻, I⁻) and Fe([15]pyaneN₅)(X)₂⁺ (X: Cl⁻, Br⁻, N₃⁻) can be explained by means of eq 4–16. Equation 4 represents a

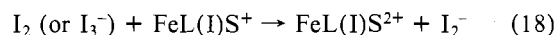


(29) Irradiations of Fe([15]pydieneN₅)(N₃)₂⁺ or Fe([15]pyaneN₅)(N₃)₂⁺ in deaerated acetonitrile produce nitrogen. However, no such a product was obtained for irradiations of the complexes in the presence of alkenes. These results suggest that 99.0% or more of the photoreactivity is a photodissociation into azide radicals. Nitrene formation must be less than or equal to the detection limit in these experiments, ~1.0%.



primary process where geminate radical-ion pairs are formed from a charge-transfer ligand to metal ($\text{X}^- \rightarrow \text{Fe(III)}$) excited state. In addition, subsequent processes, eq 5–9, show the dissociation and recombination of the geminate and solvent-separated radical-ion pairs.^{30–32} Similar reactions of caged species have been proposed for the photochemistries of other iron(III) complexes.¹

The reoxidation of the iron(II) products is very fast in case of the chlorine and bromine radicals.^{27,33} Therefore, no permanent photochemistries are detected in the absence of appropriate scavengers.³³ The small amount of photochemistry exhibited by Fe([15]pydieneN₅)(N₃)₂⁺ in flash irradiations (Figure 4b) can be attributed, by contrast with corresponding complexes of the chloride and bromide ligands, to the disproportionation of the azido radicals into nitrogen.^{29,34} However, the accumulation of the iron(II) product is noticeable even for the small concentrations produced in flash photolyses (see Figure 4). In this regard, the long-lived transient absorbances, observed in flash photolysis of Fe([15]pydieneN₅)Br₂⁺ in 0.1 M Br⁻ or Fe([15]pydieneN₅)(NCS)₂⁺, must be regarded as intermediates of the oxidation of iron(II) products by halogen or pseudohalogen molecules (see ref 27 and Figure 5). This is also demonstrated by results that have been obtained in flash irradiations of Fe([15]pydieneN₅)I₂⁺. Indeed, the amount of 680-nm absorbance, bleached at zero time (Figure 6), agrees with a formation of the products throughout competitive channels indicated by eq 10–16 (see also Appendix I). In addition, the fast decay of the transient absorbance at 780 nm (Figure 6) can be attributed to a relaxation of equilibria between various iron(II) species, namely, Fe([15]pydieneN₅)I_n(S)_{2-n}⁽²⁻ⁿ⁾⁺ with $n = 0, 1, \text{ or } 2$. Such a relaxation must be followed by a slower outer-sphere (eq 16–18) and/or inner-sphere (eq 16, 17, 19–21) redox reactions of the iron(II) complex with I₂ and I₃⁻ (see Appendix I).³³



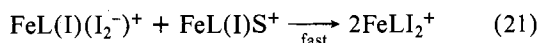
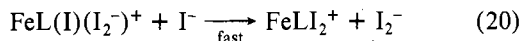
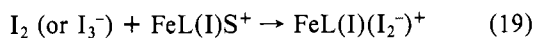
(30) Primary and solvent-separated radical-ion pairs are represented by $\{\text{FeL(X)}^+, \text{X}^\bullet\}$ and $\{\text{FeL(X)}\text{S}^+, \text{X}^\bullet\}$. For a detailed description of these species see ref 31 and 32 and references therein.

(31) Endicott, J. F. In "Concepts in Inorganic Photochemistry": Adamson, A. W., Fleischauer, P. D., Eds.; Wiley: New York, 1975.

(32) Endicott, J. F.; Ferraudi, G. J.; Barber, J. R. *J. Phys. Chem.* **1975**, 79, 630.

(33) Redox reactions of iron(II) complexes with free radicals are known to be fast processes. Moreover, these reactions can proceed by either or both of inner- and outer-sphere pathways: Buxton, G. C.; Sellers, R. M. *Coord. Chem. Rev.* **1977**, 22, 195; Thornton, A. T.; Lawrence, G. S. *J. Chem. Soc., Dalton Trans.* **1973**, 804.

(34) The photoredox behavior of the iron(III) complexes seems to be similar to that reported for Co(CN)₅X³⁻ (X: Cl⁻, Br⁻, N₃⁻, I⁻): Ferraudi, G.; Endicott, J. F. *J. Am. Chem. Soc.* **1973**, 95, 2371; *Inorg. Chem.* **1973**, 12, 2389.



The photochemical reactivity of the iron(III) complexes of the [15]pydieneN₅ and [15]pyaneN₅ ligands must be attributed to the population of the ligand to metal (X⁻ → Fe(III)) charge-transfer states, CTTM in eq 4. This is in agreement with a previous assignment of intense visible-ultraviolet absorptions to charge-transfer transitions.^{22,23,35} Indeed, values for the optical electronegativities of the iron(III), obtained from the position of these absorptions, are in agreement with those reported for other high-spin iron(III) species.³⁶ Also, the energies for threshold and maximum absorptions, E_{ab}^{th} and E_{ab}^{max} , show a dependence on the electroaffinity of the radical X⁻ that can be attributed to the charge-transfer nature of the excited state (see Table III). In this regard a large contribution to E_{ab}^{th} and E_{ab}^{max} must be associated with the energy for a transfer of the charge from the axial ligand X⁻ to the metal center (see below).

The difference between the energies for threshold and maximum absorptions, $E_{ab}^{\text{max}} - E_{ab}^{\text{th}}$ in Table III, can be related with distinct configurations for the excited and ground states. This must involve Franck-Condon contributions, associated with variations in metal-ligand distances, and reorientation of the solvent molecules. Such contributions have been already considered in connection with the photochemistry of cobalt(III) complexes.^{31,32} In this regard, the constant value, $E_{ab}^{\text{max}} - E_{ab}^{\text{th}} \approx 9$ kcal/mol (see Table III), suggests that the Franck-Condon contributions are the same for different members of the [15]pydieneN₅ and [15]pyaneN₅ series.

The threshold energy for photochemical reactivity, $E_{\text{phot}}^{\text{th}}$, increases almost linearly with the electroaffinity of the radical X⁻ (Figure 8). This behavior can be related to contributions to $E_{\text{phot}}^{\text{th}}$ which are originated in the oxidation of the axial ligand.³⁷ Moreover, transfer of the charge to the metal-centered orbitals can leave the iron with distinct electronic configurations.³⁸ Configurations obtained when bonding orbitals of the iron(III) are populated will impart some bonding character to the charge-transfer state.³⁹ The difference $E_{\text{phot}}^{\text{th}} - E_{\text{abs}}^{\text{th}}$ can be used as a qualitative measure of the bonding character within the series of complexes. Several other contributions, energies from Franck-Condon factors and changes

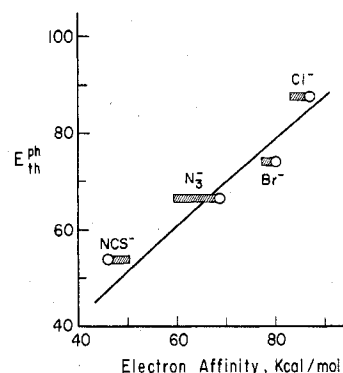


Figure 8. Dependence of the threshold energy for photochemistry on the electroaffinity of the radical X⁻ in photolyses of Fe([15]pydieneN₅)(X)₂⁺. For values of the radical's electroaffinity, see footnote b in Table III.

in LFSE and solvent repolarization, are expected to determine the value of $E_{\text{phot}}^{\text{th}} - E_{\text{abs}}^{\text{th}}$.

The nature of the equatorial ligand has a large influence on the energies of the redox processes. Indeed, the dependence of the redox potentials on the macrocycle ligand has been previously reported by Busch et al.⁴⁰ This is also observed with complexes of [15]pydieneN₅ and [15]pyaneN₅, where differences of 6 kcal/mol have been determined between the redox potentials (Table I). Moreover, a comparison of the threshold energies for photochemistry obtained with homologous [15]pydieneN₅ and [15]pyaneN₅ complexes (Table III) shows differences of 20 kcal/mol between each other. This influence of the equatorial ligand on the ground- and excited-state redox properties can be attributed to either one difference or both differences in LFSE and Franck-Condon factors.³⁷⁻³⁹ However, differences in the Franck-Condon contributions, associated with these macrocycles, are not expected to present large differences (see above). In this regard, it seems that this effect must be related with distinct LFSE contributions.

Conclusions

Results, obtained throughout this work, show that the photochemistries of the iron(III) complexes of the macrocycles [15]pydieneN₅ and [15]pyaneN₅ are largely dependent on the axial ligand. Indeed, this is expected for processes in ligand to metal, X⁻ → Fe(III), charge-transfer states. Also, the photochemical process is largely influenced by equatorial ligands. The effect(s) of the medium remains (remain) to be probed in future work.

Although no positive evidence has been obtained for photosubstitution of the ligands in axial positions or photooxidation of the equatorial ligand, the possibility of these processes cannot be neglected in other iron(III) macrocyclic species.

Acknowledgment. The research described herein was supported by the Office of Basic Energy Sciences of the Department of Energy. This is Document No. 1969 from the Notre Dame Radiation Laboratory.

This author is indebted to Mr. R. Steinback and Mr. V. R. Bhagat for their assistance in building the cyclic voltammetry setup. Helpful discussions with Dr. Endicott are also acknowledged.

Appendix I

The results, obtained in flash photolyses of Fe([15]pydieneN₅)I₂⁺, represented by FeI⁺, were analyzed according to a simplified reaction scheme, eq 22-27. Reactions 22-24 are

(35) Notice that the absorption spectrum can be originated in ligand-centered transitions for wavelengths equal to or smaller than 260 nm.

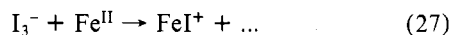
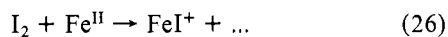
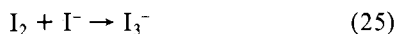
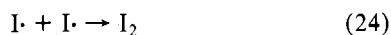
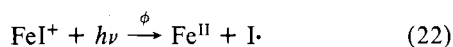
(36) Optical electronegativities, $\chi_{\text{opt}} \approx 2.2$, were obtained for high-spin iron(III) complexes of the [15]pydieneN₅ or [15]pyaneN₅ ligands. These values were calculated according to: Jørgensen, C. K. *Solid State Phys.* **1962**, *13*, 376; *Mol. Phys.* **1963**, *6*, 43.

(37) In a first-order approximation (as in: Mulliken, R. S. *J. Am. Chem. Soc.* **1952**, *74*, 811) the energy e of a charge-transfer transition can be represented by³² $E = (I + \Delta_1) + \epsilon_x + (\text{SPE}) + \Delta Q + \Delta S + \dots$, where the vertical ionization potential of the metal ion, I , is perturbed by given ligand field energies, Δ_1 , ϵ_x is the vertical electron affinity of the radical formed in the charge-transfer oxidation of the ligand, ΔQ and ΔS are energies which account for Franck-Condon and solvent reorganization contributions in nonvertical transitions between ground and charge-transfer states, and (SPE) is the change in spin-pairing energies between the configurations of the ground and excited states.

(38) The microsymmetry of the [15]pydieneN₅ and [15]pyaneN₅ complexes was considered to be D_{5h} in a first approximation.²⁴ The electronic configuration $(e_1'')^2(a_1')^2(e_2'')^2$ is expected for iron(III) in these high-spin complexes. Transfer of charge from ligand-centered orbitals with σ or π symmetry to metal-centered orbitals will introduce the following changes in ligand field stabilization energy (LFSE), Δ_1 : (a) transfer to e_1'' , $\Delta_1 = -6.42D_{xy} + 0.57D_z$; (b) transfer to a_1' , $\Delta_1 = -5.35D_{xy} + 5.14D_z$; (c) transfer to e_2'' , $\Delta_1 = 9.10D_{xy} - 3.14D_z$. The parameters D_{xy} and D_z are the equatorial and axial contributions to the ligand field. The expressions for Δ_1 contemplate the change of the average field in the excited state.

(39) Notice the increase in stability, Δ_1 , that is associated with a change in LFSE when charge is transferred to e_1'' metal-centered orbitals.

(40) Dabrowiak, J. C.; Lovecchio, F. V.; Goedken, V. L.; Busch, D. H. *J. Am. Chem. Soc.* **1972**, *94*, 5502.



very fast and take place during the flash irradiation. In this regard, the bleach of the absorbance at $\lambda \sim 700$ nm can be attributed to a rapid disappearance of FeI^+ .

The disappearance of FeI^+ is described by eq 28, where I_0

$$-d[(\text{FeX}^+)/dt] = -\phi I_0 + k_{23}[\text{Fe}^{\text{II}}][\text{I}\cdot] \quad (28)$$

is the absorbed-light intensity and k_{23} the rate constant of eq 23. A solution for eq 28 was obtained by using average concentrations of Fe^{II} and $\text{I}\cdot$ over the irradiation period. These concentrations were proportional to the average photonic concentration, $I_0(\Delta t)$, of the flash. Moreover, the amount of FeI^+ , $\Delta[\text{FeI}^+]$, transformed during the irradiation period, Δt , is given by eq 29, where α is a proportionality constant. The

$$\Delta[\text{FeI}^+] = -\phi I_0(\Delta t) + k_{23}(\alpha I_0(\Delta t))^2(\Delta t) \quad (29)$$

number of photons produced per pulse, $I_0(\Delta t)$, is proportional to the energy of the flash, E . Therefore the amount of the absorbance, ΔA , bleached by the flash can be related to the flash energy by means of the eq 30, where a and b are pro-

$$\Delta A = aE - bE^2 \quad (30)$$

portionality constants. The experimental verification of eq 30 is reported in the text, and it can be used as a further proof of the proposed reaction mechanism.

The fate of I_2 can be described by eq 25–27. The outer-sphere reoxidation of Fe^{II} by I_2 or I_3^- , followed by a rapid anation of the oxidation product, will produce the same spectral changes that are expected for an inner-sphere oxidation. In this regard eq 22–27 give an appropriate description of the overall process.

The equilibration between I_2 and I_3^- is rapid. Therefore, the reaction rate, eq 31, can be rearranged into eq 32, where k_i is the rate constant for eq i ($i = 26, 27$) and K is the equilibrium constant of equilibrium 25.

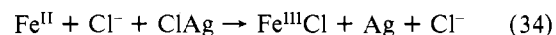
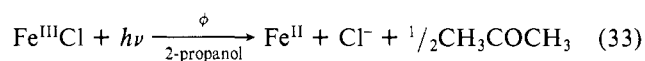
$$\frac{-d[\text{Fe}^{\text{II}}]}{dt} = k_{26}[\text{Fe}^{\text{II}}][\text{I}_2] + k_{27}[\text{Fe}^{\text{II}}][\text{I}_3^-] \quad (31)$$

$$\frac{-d[\text{Fe}^{\text{II}}]}{dt} = (k_{26} + Kk_{28}[\text{I}^-])[\text{Fe}^{\text{II}}][\text{I}_2] \quad (32)$$

The dependence of the rate constant for the recovery of the absorbance (Figure 6) agrees with eq 32.

Appendix II

The photochemical formation of the iron(II) species, eq 33, was followed by means of an electrochemical cell, $\text{Ag}|\text{ClAg}||\text{Fe}^{\text{III}}|\text{Fe}^{\text{II}}$ (eq 34). The shift of the cell reaction, eq 34,



produces an electrochemical potential which is given by the Nernst equation, eq 35. The rate of formation of iron(II)

$$\Delta V = \Delta V^\circ - 0.06 \log \frac{[\text{Fe}^{\text{III}}\text{Cl}]}{[\text{Fe}^{\text{II}}][\text{Ag}^+]} \quad (35)$$

species, $\phi I_0 t$, the potential of the reference electrode, V_r , and the initial concentration of the iron(III) complex can be introduced into the Nernst equation. These modifications show that the electrochemical potential must have a linear dependence on the logarithm of the irradiation time, eq 36.

$$\Delta V = \left([V_r - V^\circ_x] - 0.06 \log \frac{c}{\phi I_0} \right) - 0.06 \log t \quad (36)$$

The functional time dependence of eq 36 was verified throughout this work (see Figure 7). The slope, obtained from Figure 7, was 0.058 as expected for a one-electron reaction. Moreover, the intercept (0.180 V for $c = 2.0 \times 10^{-4}$ M), $\phi = 0.0340$, and $I_0 = 3.7 \times 10^{-4}$ einstein/(L·min) gave a potential $V^\circ_x = 0.25$ V for the $\text{Fe}([\text{15}]\text{pydieneN}_3)\text{Cl}_2^+|\text{Fe}([\text{15}]\text{pydieneN}_3)\text{Cl}_2$ couple. This potential and a value obtained from cyclic voltammetry (Table I) are in agreement.

Registry No. $[\text{Fe}([\text{15}]\text{pydieneN}_3)(\text{Cl})_2]\text{ClO}_4$, 25549-55-7; $[\text{Fe}([\text{15}]\text{pydieneN}_3)(\text{Br})_2]\text{ClO}_4$, 25684-58-6; $[\text{Fe}([\text{15}]\text{pydieneN}_3)(\text{I})_2]\text{ClO}_4$, 25549-56-8; $[\text{Fe}([\text{15}]\text{pydieneN}_3)(\text{NCS})_2]\text{ClO}_4$, 25684-59-7; $[\text{Fe}([\text{15}]\text{pyaneN}_3)(\text{Cl})_2]\text{ClO}_4$, 71882-24-1; $[\text{Fe}([\text{15}]\text{pyaneN}_3)(\text{Br})_2]\text{ClO}_4$, 71882-25-2; $[\text{Fe}([\text{15}]\text{pyaneN}_3)(\text{N}_3)_2]\text{ClO}_4$, 71882-26-3; $[\text{Fe}([\text{15}]\text{pydieneN}_3)(\text{Cl})_2]^+$, 47245-49-8; $[\text{Fe}([\text{15}]\text{pydieneN}_3)(\text{Br})_2]^+$, 47245-46-5; $[\text{Fe}([\text{15}]\text{pydieneN}_3)(\text{N}_3)_2]^+$, 48214-48-8; $[\text{Fe}([\text{15}]\text{pydieneN}_3)(\text{NCS})_2]^+$, 47511-51-3; $[\text{Fe}([\text{15}]\text{pydieneN}_3)(\text{I})_2]^+$, 47245-52-3; $[\text{Fe}([\text{15}]\text{pyaneN}_3)(\text{Cl})_2]^+$, 54325-45-0; $[\text{Fe}([\text{15}]\text{pyaneN}_3)(\text{Br})_2]^+$, 54340-22-6; $[\text{Fe}([\text{15}]\text{pyaneN}_3)(\text{N}_3)_2]^+$, 54325-51-8; $[\text{Fe}([\text{15}]\text{pydieneN}_3)(\text{N}_3)_2]\text{ClO}_4$, 41851-19-8; $[\text{Fe}_2([\text{15}]\text{pydieneN}_3)_2\text{O}](\text{ClO}_4)_4$, 71882-22-9.

Supplementary Material Available: Table II with quantum yields and Figure 4 with information on the transient absorbances (11 pages). Ordering information is given on any current masthead page.